STEERING TRAJECTORY ANALYSIS OF PLANETARY EXPLORATION ROVERS BASED ON ALL-WHEEL DYNAMICS MODEL

Genya Ishigami, Akiko Miwa and Kazuya Yoshida

Department of Aerospace Engineering, Tohoku University
Aoba 6-6-01, Sendai, 980-8579, JAPAN
{*ishigami, miwa, yoshida*}*@astro.mech.tohoku.ac.jp*

ABSTRACT

This paper describes a steering trajectory analysis for planetary exploration rovers. Analysis of the steering trajectory is an important issue in order to plan and control the motion maneuvers of a planetary rover. Since a rover might easily slip and skid on loose soil, it is difficult to estimate and analyze the motion of the rover or the behavior of its wheels. The authors developed a model that respects the dynamics of each wheel's slip and skid behavior in order to deal with the steering trajectory of the rover. The developed model is called *All-Wheel Dynamics Model*. In the all-wheel dynamics model, the behavior of each wheel on loose soil is modeled based on terramechanics. The steering trajectory of the rover is obtained by a numerical simulation using the wheel-and-vehicle dynamics model. The proposed model is able to correspond to the experimental results with reasonable precision.

1. INTRODUCTION

There has been an increasing number of space missions dedicated to planetary surface exploration using mobile robots (*Rovers*). The planetary rovers are expected to play a significant tasks to expand the exploration areas, increasing the scientific return of the mission. Also, the rovers are required to travel longer distances and perform more complex tasks in order to accomplish more challenging mission goals than ever. In the last decade, extensive researches have been done in various aspects for the development of planetary rovers [1]-[14].

A rover has to have enough capabilities to travel on such highly challenging terrain, climbing hills, traversing slopes, and negotiating with craters, boulders, rocks or stones spread over the terrain. The surface terrain of a planetary body such as Mars or the Moon is mostly covered with loose soil called *regolith*. On loose soil, the wheels of the rover easily slip and loose their traction. On the other hand, on rocky surface, the rover might become unstable or, in the worst case, tip over. Thus, it is necessary to investigate the static and dynamic behavior of the rover, taking into account the interaction between the wheels and the soil. Additionally, there is a strong demand to develop a validated model for an analysis of the rover's behavior.

The research field dealing with the soil mechanics is called *terramechanics*. In this field, the analysis of a wheel-soil interaction mechanism and the modeling of the stress distribution underneath the wheel have been well studied [5]-[7][14]. For instance, Iagnemma et al. successfully applied those terramechanics models to the issues of planetary robotics, and developed an on-line method to identify soil parameters (cohesion stress and friction angle) using onboard sensory data [8][9]. Jain et al. established a physics-based simulator for a planetary surface exploration rover. The simulator considers he terrain environment and the terrain/vehicle interactions [10]. We have also investigated the wheel-soil interaction for the modeling and control of a rover with taking a terramechanics-based approach [11]-[13].

This paper investigates the steering trajectory analysis of the planetary exploration rovers. The behavior of the rover might dynamically change because the wheels will easily slip or skid on the loose soil. The analysis of the steering trajectory becomes a comparatively complicated issue by such dynamic behavior. The main focus of this paper, therefore, is the development of a better analysis model for the rover that respects each wheel's behavior on loose soil. We call the model *All-Wheel Dynamics Model* since it implies the dynamics of all wheels. The all-wheel dynamics model consists of two models; one is a wheel-soil contact model, and the other is a rover-dynamics model (Fig.1.)

The wheel-soil contact model is a key issue for the all-wheel dynamics model. The basic study of the contact model for a rigid wheel on loose soil has been studied in the terramechanics field, as mentioned above. However, the investigation for the lat-

Proc. of 'The 8th International Symposium on Artifical Intelligence, Robotics and Automation in Space - iSAIRAS', Munich, Germany.
5-8 September 2005, (ESA SP-603, August 2005)

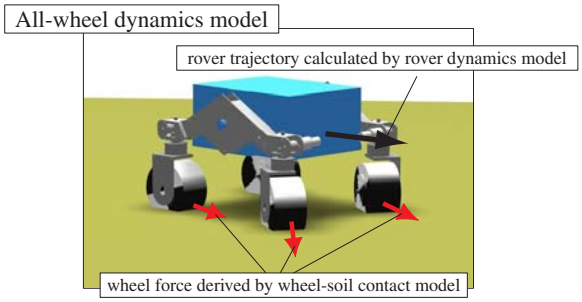

Fig. 1. Concept of the all-wheel dynamics model

eral (side) forces of the wheel on loose soil has been left as an open issue. The modeling of the side force is absolutely necessary in order to address the steering trajectory. We, therefore, have proposed the contact model including the side forces that gives good approximations [13]. Then, in this paper, the wheel-soil contact model is discussed to apply itself to both a horizontal and an inclined (slope) surface. A dynamic behavior of the wheel is characterized by two parameters; one is slip ratio and the other is slip angle. The proposed model uses these parameters as a state variable of the wheel.

We also establish the rover-dynamics model as an articulated body system. By the use of the wheel-soil contact model, forces from soil to each wheel is able to be calculated. The dynamics simulation using the all-wheel dynamics model derives the steering trajectory of the rover. The steering trajectories obtained from the simulation are compared to the corresponding experimental trajectories of our rover test bed.

This paper is organized as follows. The following section (Section 2) introduces the wheel-soil contact model, particularly, the modelling of the side force. In Section 3, the proposed all-wheel dynamics model is elaborated. Section 4 deals with the analyses of the steering trajectory using the proposed model. The steering trajectory obtained by the all-wheel dynamics model is compared with the experimental results. Then, the validity of the proposed model is confirmed. Also, different steering trajectories are simulated with different steering angles when the rover traverses a slope, then steering maneuvers on a slope traverse are discussed.

2. WHEEL-SOIL CONTACT MODEL

The following analysis deals with a rigid wheel rotating on loose soil. A wheel coordinate system is defined using a right-hand frame as shown in Fig.2, where the longitudinal direction is denoted by x, the lateral direction by y, and the vertical direction by z. The coordinate frame turns according to the steering action of the wheel (the yaw rotation around z axis), but does not rotate with the driving motion of the wheel (the pitch rotation around y axis).

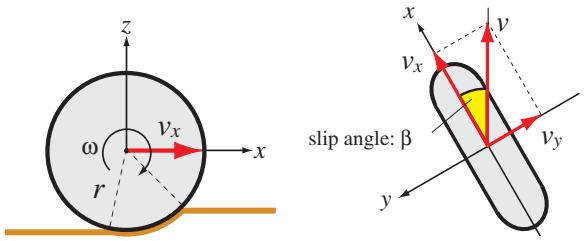

Fig. 2. Wheel coordinate system

2.1 Slip ratio and Slip angle

When a wheel travels on a loose soil, the wheel can slip both in the longitudinal and lateral directions. The slip in the longitudinal direction is measured by "slip ratio," which is defined as a function of the longitudinal traveling velocity v_x and the circumference velocity of the wheel $r\omega$:

$$s = \begin{cases} (r\omega - v_x)/r\omega & (r\omega > v_x : \text{driving}) \\ (r\omega - v_x)/v_x & (r\omega < v_x : \text{braking}) \end{cases} \tag{1}$$

The slip ratio takes a value between -1 and 1.

On the other hand, the slip in the lateral direction is measured by "slip angle," which is defined by the longitudinal and lateral traveling velocities v_x, v_y:

$$\beta = \tan^{-1}(v_y/v_x) \tag{2}$$

2.2 Wheel stress distribution

Based on the terramechanics approach, a stress distribution of the wheel can be described as shown in Fig.3. The normal stress $\sigma(\theta)$ is modeled according to [11]-[13]:
when $\theta_m \le \theta \le \theta_f$:

$$\sigma(\theta) = \sigma_m \cdot \left(\frac{\cos\theta - \cos\theta_f}{\cos\theta_m - \cos\theta_f} \right)^n \tag{3}$$

when $\theta_r \le \theta \le \theta_m$:

$$\sigma(\theta) = \sigma_m \cdot \left(\frac{\cos\{\theta_f - \frac{\theta-\theta_r}{\theta_m-\theta_r}(\theta_f - \theta_m)\} - \cos\theta_f}{\cos\theta_m - \cos\theta_f} \right)^n \tag{4}$$

θ_m is the specific wheel angle at which the normal stress is maximized:

$$\theta_m = (a_0 + a_1 s)\theta_f \tag{5}$$

where a_0 and a_1 are soil specific parameters. The values of them are generally assumed as $a_0 \approx 0.4$ and $0 \le a_1 \le 0.3$ [14].

The maximum stress σ_m is given by [7]:

$$\sigma_m = r^n \left(\frac{k_c}{b} + k_\phi \right) (\cos\theta_m - \cos\theta_f)^n \tag{6}$$

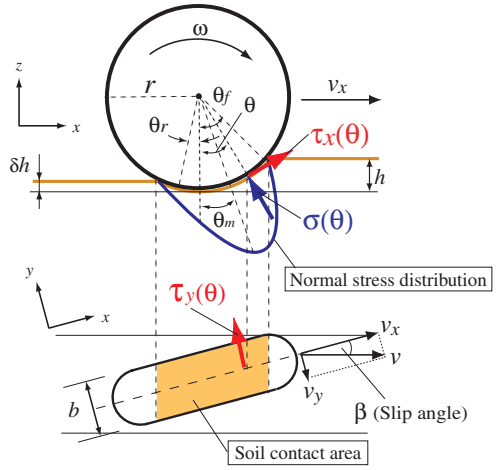

Fig. 3. Stress distribution of the wheel on loose soil

where, k_c, k_ϕ and n are also the soil-specific parameters. b is the width of the wheel.

The longitudinal and lateral shear stresses $\tau_x(\theta)$ and $\tau_y(\theta)$ are written by the same expression:

$$\tau_i(\theta) = (c + \sigma(\theta)\tan\phi)\{1 - e^{-j_i/k_i}\}, \ (i = x, y) \quad (7)$$

The symbols used in the equation (7) are listed as follows:

c : cohesion stress of the soil
ϕ : internal friction angle of the soil
k_i : shear displacement in each direction (i=x, y)

Also, j_x and j_y indicate soil deformations in each direction, which are formulated as a function of the wheel angle θ:

$$j_x(\theta) = r\{\theta_f - \theta - (1-s)(\sin\theta_f - \sin\theta)\} \quad (8)$$
$$j_y(\theta) = r(1-s)(\theta_f - \theta)\cdot\tan\beta \quad (9)$$

2.3 Modeling of wheel forces

A general force model for a rigid wheel on loose soil is shown in Fig.4.

Drawbar pull F_x

The drawbar pull F_x is a net traction force generated at the longitudinal direction of the wheel. By the uses of the normal stress $\sigma(\theta)$ and the shear stress in x direction $\tau_x(\theta)$, a drawbar pull F_x that exerts from the soil to the wheel is calculated by the integral from the entry angle θ_f to the exit angle θ_r [5]-[7]:

$$F_x = rb\int_{\theta_r}^{\theta_f}\{\tau_x(\theta)\cos\theta - \sigma(\theta)\sin\theta\}d\theta \quad (10)$$

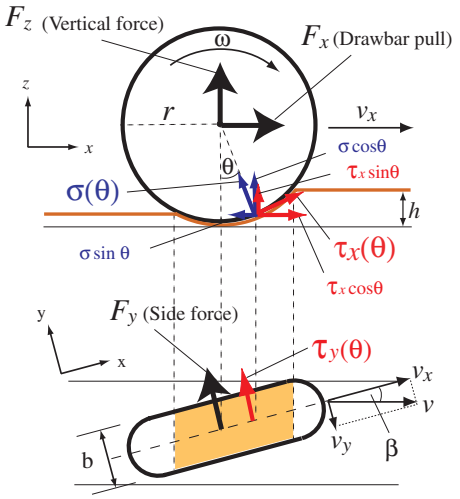

Fig. 4. Force model of the wheel on loose soil

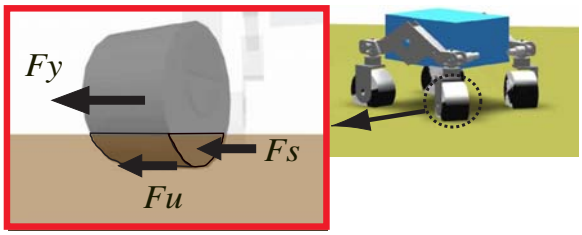

Fig. 5. Lateral (side) forces acting on the wheel

Side force F_y

Side force F_y appears at the lateral direction of the wheel when the wheel or the vehicle makes a steering. We have modeled the side force as follows [13]:

$$F_y = F_u + F_s \quad (11)$$

As shown in Fig.4 and Fig.5, F_u is a force produced by the shear stress in y direction $\tau_y(\theta)$ underneath the wheel. F_s is a reaction force generated by a bulldozing phenomenon on a side face of the wheel.

Then, equation (11) can be rewritten as:

$$F_y = \int_{\theta_r}^{\theta_f}\{\underbrace{rb\cdot\tau_y(\theta)}_{F_u} + \underbrace{R_b\cdot(r - h(\theta)\cos\theta)}_{F_s}\}d\theta \quad (12)$$

We applied *Hegedus's bulldozing resistance estimation* in order to derive the force F_s. As descried in Fig.6, a bulldozing resistance R_b is generated to an unit width blade when the blade moves towards the soil. According to the Hegedus's theory, the bulldozing area is defined by a destructive phase which is modeled by a planar surface and the swelled ground which is generated on the soil surface. In the case of a horizontally placed wheel, an angle of approach α' should be zero. Then, R_b can be calculated as a

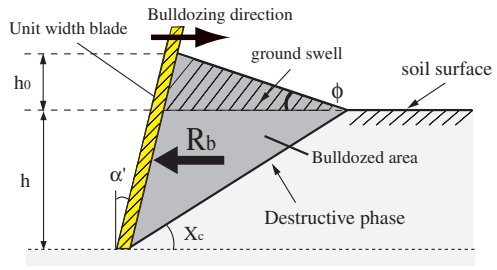

Fig. 6. Estimation model of the bulldozing resistance

function of a wheel sinkage h:

$$R_b(h) = D_1 \cdot (c \cdot h + \rho D_2 \cdot h^2/2) \quad (13)$$

where,

$$D_1(X_c, \phi) = \cot X_c + \tan(X_c + \phi) \quad (14)$$
$$D_2(X_c, \phi) = \cot X_c + \cot^2 X_c / \cot \phi \quad (15)$$

In the above equations, ρ means a soil density. The wheel sinkage h is given as a function of wheel angle θ [11]-[13]:

$$h(\theta) = r(\cos\theta - \cos\theta_f) \quad (16)$$

Also, based on Bekker's theory [6], the destructive angle X_c can be approximated as:

$$X_c = 45^\circ - \phi/2 \quad (17)$$

Vertical force : F_z

The vertical force F_z is obtained by the same fashion of equation (10) [5]-[7]:

$$F_z = rb \int_{\theta_r}^{\theta_f} \{\tau_x(\theta)\sin\theta + \sigma(\theta)\cos\theta\} d\theta \quad (18)$$

The vertical force should be equal to the normal load of the wheel.

2.4 Wheel model on inclined surface

We have applied the wheel-soil contact model to the inclined surface as shown in Fig.7.

In the case of the inclined surface, the definition of the wheel coordinate system $\{\Sigma_w\}$ is considered to be equal to the horizontal case. The inclined surface is assumed to be uniform, and the slope angle is denoted by α. When an inertial coordinate system is expressed by $\{\Sigma_0\}$ as a right-hand system, the direction, which is parallel to the traverse direction of the slope, is denoted by x_0, and the vertical direction by z_0.

The coordinate transformation from $\{\Sigma_0\}$ to $\{\Sigma_w\}$ is employed by a rotation of x_0 axis with α, then another rotation of z_0 axis with γ. The angle composed between x_0-y_0 planar surface and x (or y) axis is determined by Φ (or Ψ).

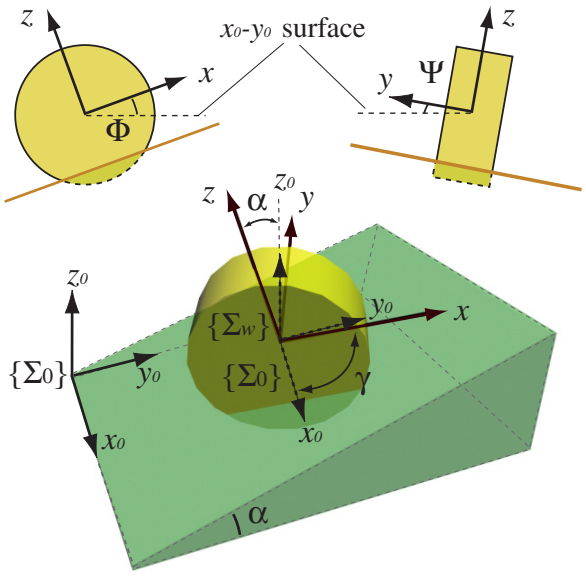

Fig. 7. Definition of the wheel coordinate (Inclined surface)

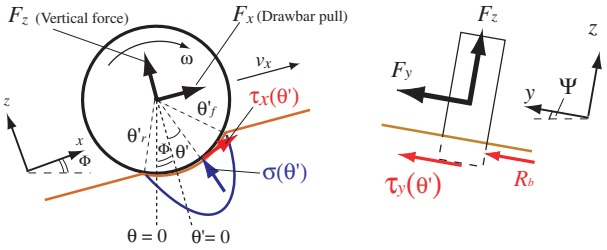

Fig. 8. Force model of the wheel (Inclined surface)

Wheel forces on inclined surface

As shown in Fig.8, the wheel angle θ' is given by $\theta' = \theta - \Phi$, and also θ' is supposed to be zero in the normal direction of the inclined surface. Note that, the stress distribution is assumed to be equivalent to the case of the horizontal surface, not dependent to Φ and Ψ.

Using θ' instead of θ, forces of the wheel in the case of the inclined surface are derived in the same fashion as equations (10), (12) and (18).

$$F_x = rb \int_{\theta'_r}^{\theta'_f} \{\tau_x(\theta')\cos\theta' - \sigma(\theta')\sin\theta'\} d\theta' \quad (19)$$

$$F_y = \int_{\theta'_r}^{\theta'_f} \{rb \cdot \tau_y(\theta') + R_b \cdot (r - h(\theta')\cos\theta'\} d\theta' \quad (20)$$

$$F_z = rb \int_{\theta'_r}^{\theta'_f} \{\tau_x(\theta')\sin\theta' + \sigma(\theta')\cos\theta'\} d\theta' \quad (21)$$

Fig. 9. Rover test bed

3. ALL-WHEEL DYNAMICS MODEL

The all-wheel dynamics model is developed in order to analyze the steering trajectory of the planetary rover. Using the wheel-soil contact model as mentioned in Section 2, the contact forces of each wheel can be calculated.

3.1 Rover test bed

In this paper, the rover-dynamics model refers to a rover test bed which we developed. The 4-wheeled rover test bed, shown in Fig.9, has the dimension of 0.62 [m](length) × 0.53 [m](width) × 0.46 [m](height) and weighs about 35 [kg] in total. Each wheel, in diameter of 0.18 [m], is made of aluminum covered with paddles of 0.01 [m] heights. All wheels have active steering DOF (Degree Of Freedoms). The wheels are connected to the main body by a rocker suspension. The rocker is a non-spring passive suspension mechanism to connect wheels by free-pivot links. This differential link is used to keep the pitch angle of the main body in the middle of the left and right rocker angles.

3.2 Rover dynamics model

A dynamics model of the rover shown in Fig.10 is completely equivalent to the rover test bed.

A rover's coordinate system of the main body is defined $\{\Sigma_b\}$. A longitudinal direction of the body is denoted by x_b, normal direction of the rover by z_b.

The dynamic motion equation of the rover is generally written as:

$$\mathbf{H}\begin{bmatrix}\dot{\mathbf{v}}_0\\ \dot{\omega}_0\\ \ddot{\mathbf{q}}\end{bmatrix}+\mathbf{C}=\begin{bmatrix}\mathbf{F}_0\\ \mathbf{N}_0\\ \tau\end{bmatrix}+\mathbf{J}^T\begin{bmatrix}\mathbf{F}_e\\ \mathbf{N}_e\end{bmatrix} \qquad (22)$$

where the symbols used in the above equation are listed as:

- $\mathbf{H}$: inertia matrix of the rover
- $\mathbf{C}$: velocity depending term
- $\mathbf{v}_0$: translational velocity of the body
- ω_0 : angular velocity of the body

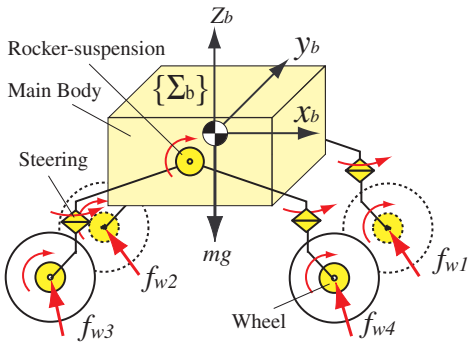

Fig. 10. Rover dynamics model

- $\mathbf{q}$: angle of each joint of the rover
- $\mathbf{F}_0$: forces acting at the center of gravity of the body
- $\mathbf{N}_0$: torques acting at the center of gravity of the body
- τ : torques acting at each joint of the rover
- $\mathbf{J}$: Jacobian matrix
- $\mathbf{F}_e = \left[f_{w1}^T, \cdots, f_{wm}^T\right]^T$: external forces acting at the center of gravity of each wheel
- $\mathbf{N}_e$: torques acting at the center of gravity of each wheel

Note that, each external force $f_{wi}(i = 1, \cdots, m)$ is derived by the wheel-soil contact model, as mentioned in Section 2. Here, m is the number of wheels.

The above equations are general and can be applied to a vehicle with any configuration. Specific parameters for the rover kinematics and dynamics are identified from the test bed and used in the simulation. The trajectory of the rover with a given traveling and steering conditions is numerically obtained by solving the equation (22) successively.

3.3 Simulation procedure

The simulation procedures using the all-wheel dynamics model are summarized as follows:

1. Input steering angles δ_{wi} and angular velocities ω_{wi} at each wheel ($i = 1, \cdots, 4$, in this case).
2. Calculate external forces f_{wi} acting at each wheel using the wheel's contact model.
3. Determine $\mathbf{F_0}$, $\mathbf{N_0}$, $\mathbf{F_e}$, $\mathbf{N_e}$ and τ.
4. Solve equation (22), then obtain the rover's position, orientation and velocity.
5. Calculate slip ratios and slip angles of each wheel, then return to 2).

The simulation was performed by using an in-house software, named *SpaceDyn*. The *SpaceDyn* is a MATLAB toolbox that solves numerical computations of kinematics and dynamics of the articulated body systems with a moving base [15][16]. We used it

Table 1. Soil specific parameters and values

parameter	value	unit
r	0.09	[m]
b	0.11	[m]
a_0	0.40	
a_1	0.15	
c	0.80	[kPa]
ϕ	37.2	[deg]
k_x	$0.014 \sim 0.023$	[m]
k_y	$0.016 \sim 0.022$	[m]
k_c	1.37×10^3	$[\mathrm{N/m^{n+1}}]$
k_ϕ	8.14×10^5	$[\mathrm{N/m^{n+2}}]$
n	1.0	

to obtain the forward dynamics solution of equation (22).

The soil specific parameters used in the simulations are listed in Table 1. The values of those parameters were identified from other experiments [12].

4. STEERING TRAJECTORY ANALYSIS

We conducted two analyses; 1) the rover travels on a horizontal surface, and 2) traverses an inclined surface. The former analysis deals with the comparison between the simulation and experimental results. The latter one gives slope traverse simulations with different steering angles.

4.1 Analysis-1 : Horizontal surface

In the following discussion of horizontal surface, we will compare the numerical results with the experimental results obtained in our rover test bed.

Steering experiments

In the steering experiments, the rover test bed travels with a given angular velocity and a steering angle. Each wheel is controlled to travel with a constant wheel angular velocity and a constant steering angle by an on-board computer. We measured a motion trajectory of the rover using a 3D optical sensor. Force/torque sensors are also mounted on upper part of each wheel to measure the forces generated by the corresponding wheel. The test field is evenly covered with the Lunar Regolith Simulant.

The experiments had two conditions as listed in Table 2; in case-a, the steering angles of the front wheels were fixed to keep 15 [deg], and in case-b to -30 [deg]. The steering angles of the rear wheels were 0 [deg] in both conditions. In the experiments, the given angular velocity of each wheel was 12.0 [rpm]. The average traveling velocity of the rover was around 0.08 [m/s]. Overviews of the steering experiment in the case-b are shown in Fig.11.

Table 2. Simulation and experimental conditions (Horizontal surface)

Case	Steering angle [deg]	
	Front wheels	Rear wheels
a : Left turn	15	0
b : Right turn	-30	0
Wheel angular velocity	12 [rpm]	
Traveling time	15 [sec]	

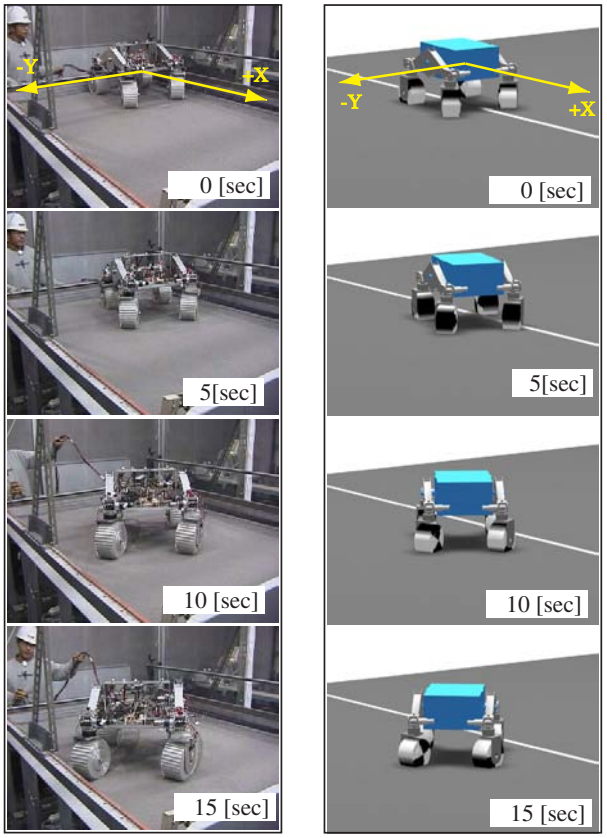

Fig. 11. Comparison of the rover's steering motion

Comparison between simulation and experiment

The experimental results of the rover's trajectory are shown in Fig.12 and Fig.13. Corresponding simulation results using the all-wheel dynamics model are also described in those figures. Fig.11 shows a computer graphics model to represent the result of the dynamics simulation in the case-b.

From Fig.12 and Fig.13, it can be seen that the trajectory obtained from the all-wheel dynamics model reproduces well the experimental result with reasonable precision. These results indicate that the all-wheel dynamics model has enough reliability to deduce the steering trajectory or the motion of the rover.

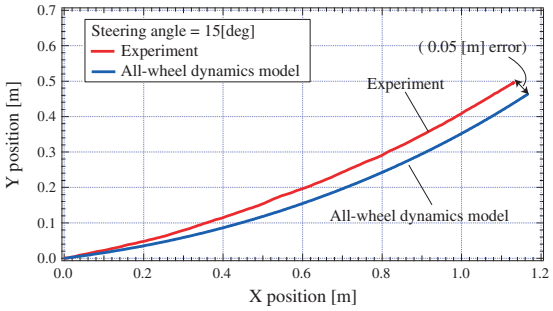

(Case-a : front=15 [deg], rear=0 [deg])

Fig. 12. Steering trajectories on horizontal surface

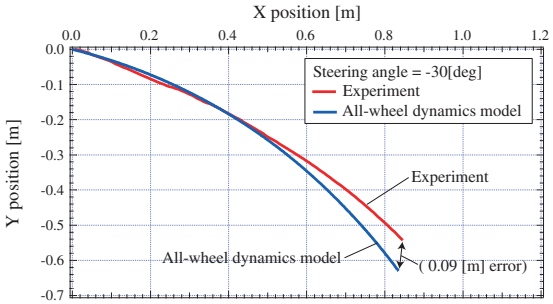

(Case-b : front=-30 [deg], rear=0 [deg])

Fig. 13. Steering trajectories on horizontal surface

Table 3. Simulation and experimental conditions (Slope traverse)

Case	Steering angle [deg]	
	Front wheels	Rear wheels
A	0	0
B	15	0
C	15	15

Wheel angular velocity	12 [rpm]
Traveling time	15 [sec]
Slope angle	10 [deg]

4.2 Analysis-2 : Slope traverse simulation

In this analysis, the wheel forces were derived by the wheel-soil contact model on inclined surface. As presented in Table 3, we used three different steering angles when the rover traverses a slope. The slope angle was 10 [deg].

Simulation results regarding the steering trajectory are shown in Fig.14. Also, Fig.15 presents the time history about the yaw orientation of the rover. Fig.16 describes behaviors of the rover by the use of the computer graphics.

In the case-A, the rover traveled toward the bottom of the slope. From Fig.15 and Fig.16, we can find that the rover did not rotate around yaw axis. Thus, in the case-A, the rover skidded and slid off the slope, then could not traverse the slope. On the other hand, in the case-B and C, the rover was able

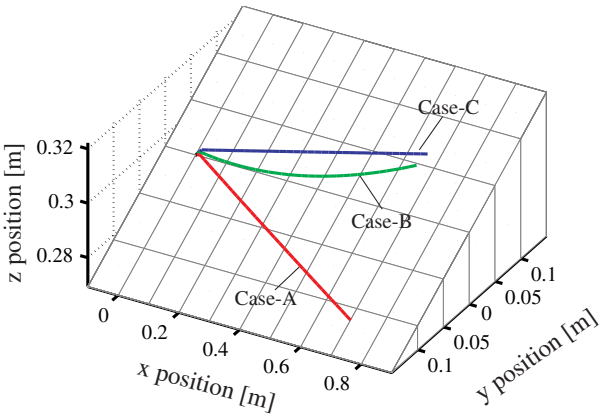

Fig. 14. Comparison of steering trajectories on slope

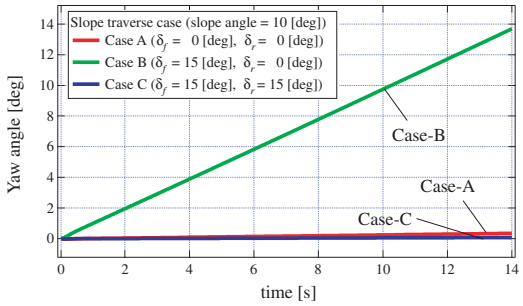

Fig. 15. Yaw angle of the rover on slope

to traverse and climb up the slope with a curved or linear trajectory, respectively. In the case-C, the rover traveled the slope without its yaw rotation. It means that the rover moved in parallel rather than steering.

These results imply that better steering angles can be obtained using the proposed model so that the rover successfully traverse a slope.

5. CONCLUSION

In this paper, the steering trajectory analysis of the planetary exploration rover was investigated. The all-wheel dynamics model, which respects to each wheel's behavior and the rover's dynamics, was developed for a better analysis of the steering trajectory.

As one of the main issues of the all-wheel dynamics model, the contact model between the rigid wheel and loose soil was also elaborated based on the terramechanics approach. The wheel-soil contact model is appropriate to describe the wheel forces when the wheel travels both on a horizontal and an inclined surface.

The proposed all-wheel dynamics model shows a good approximation that corresponds with the experimental trajectory. Additionally, from the results

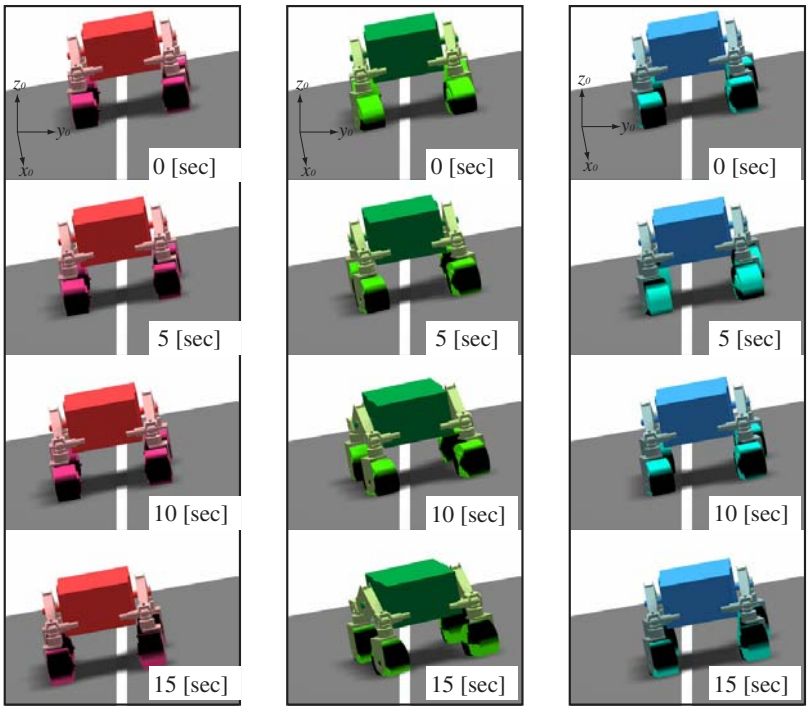

(Left figure : Case-A, Center figure : Case-B, Right figure : Case-C)

Fig. 16. Rover's behaviour on slope

of the slope traverse simulations, we can discuss how to control a steering motion in order to successfully traverse a slope, climb up a hill, and negotiate a crater.

The all-wheel dynamics model will be appropriate for future practical issues, such as planning better steering maneuvers and controlling the steering motion to follow the given trajectory.

References

[1] http://marsrovers.jpl.nasa.gov/home/index.html (as of June 2005)

[2] I. Nakatani, K. Matsumoto, T. Izumi; "SELENE-B: Proposed Lunar Mission with Lander and Rover," *Proc. of the 7th Int. Symp. on Artificial Intelligence, Robotics and Automation in Space,* 2003.

[3] R. Volpe and S. Peters; "Rover Technology Development and Infusion for the 2009 Mars Science Laboratory Mission," *Proc. of the 7th Int. Symp. on Artificial Intelligence, Robotics and Automation in Space,* 2003.

[4] K. Rajan, et. al.; "MAPGEN: Mixed Initiative Planning and Scheduling for the Mars '03 MER Mission," *Proc. of the 7th Int. Symp. on Artificial Intelligence, Robotics and Automation in Space,* 2003.

[5] M. G. Bekker; "*Introduction to Terrain-Vehicle Systems,*" The University of Michigan Press, 1969.

[6] M. G. Bekker; "*OFF-THE-ROAD LOCOMOTION,*" The University of Michigan Press, 1960.

[7] J. Y. Wong; "*Theory of Ground Vehicles,*" John Wiley & Sons, 1978.

[8] K. Iagnemma, H. Shibly, S. Dubowsky; "On-Line Traction Parameter Estimation for Planetary Rovers," *Proc. of the 2002 IEEE Int. Conf. on Robotics and Automation,* pp. 3142–3147, 2002.

[9] K. Iagnemma and S. Dubowsky,; "*Mobile Robot in Rough Terrain,*" Springer Tracts in Advanced Robotics, vol.12, 2004.

[10] A. Jain, J. Guineau, C. Lim, W. Lincoln, M. Pomerantz, G. Sohl, R. Steele "Roams: Planetary Surface Rover Simulation Environment," *Proc. of the 7th Int. Symp. on Artificial Intelligence, Robotics and Automation in Space,* 2003.

[11] K. Yoshida, T. Watanabe, N. Mizuno, G. Ishigami, "Terramechanics-Based Analysis and Traction Control of a Lunar/Planetary Rover," *4th Int. Conf. on Field and Service Robotics,* 2003.

[12] K. Yoshida, N. Mizuno, G. Ishigami, A. Miwa, "Terramechanics-Based Analysis for Slope Climbing Capability of a Lunar/Planetary Rover," *24th Int. Symp. on Space Technology and Science,* 2004.

[13] K. Yoshida, G. Ishigami; "Steering Characteristics of a Rigid wheel for Explaration on Loose Soil," *Proc of the 2004 IEEE Int. Conf. on Intelligent Robots and Systems,* pp. 3995–4000, 2004.

[14] J. Y. Wong, A. R. Reece, "*Prediction of Rigid Wheel Prefoemance Based on the Analysis of Soil-Wheel Stresses Part I, Preformance of Driven Rigid Wheels,*" Journal of Terramechanics, vol.4, 1967

[15] K. Yoshida ; "*The SpaceDyn : a MATLAB Toolbox for Space and Mobile Robots,*" J. of Robotics and Mechatronics, vol.12 no.4, pp. 411-416, 2000.

[16] http://www.astro.mech.tohoku.ac.jp/spacedyn